Integrative sampling of suspended particulate matter in rivers: assessing the grain-size dependent efficiency of passive particle traps

Céline Berni, Yann Bonenfant, Matthieu Masson, Jérôme Le Coz, Aymeric Dabrin, Fabien Thollet

Integrative sampling of suspended particulate matter in rivers: assessing the grain-size dependent efficiency of passive particle traps

Céline Berni[1*], Yann Bonenfant[1], Matthieu Masson[1], Jérôme Le Coz[1], Aymeric Dabrin[1], Fabien Thollet[1]

[1*]RiverLy, INRAE, Lyon, France.

*Corresponding author(s). E-mail(s): celine.berni@inrae.fr;

Abstract

Purpose: Passive particle traps (PTs) are cost-efficient and easy to operate tools for the time integrative monitoring of particulate contaminants in surface fresh-waters. Box-type PTs are designed as boxes through which the river flow is slowed down in order to collect Suspended Particulate Matter (SPM). However, a particle-size distribution bias in collection suggests that the finest particles pass through PTs without settling. The aim of this study is to quantify SPM trapping efficiency as a function of particle size, and to develop a predictive model.

Methods: We designed laboratory experiments using box-type PTs. The trap was either submerged in a SPM-laden flow (in-flow experiment); or directly supplied with water and SPM with a pipe connected to its inlet (in-line experiments). SPM concentration, particle-size distributions (PSD), flow velocity were controlled and recorded.

Results: In-line experiment results confirmed that coarser particles are more efficiently trapped than smaller ones due to their higher settling velocity. The particle-size trapping efficiency was regressed against PT dimensions and incoming flow velocity. The application of these results to in-flow and field experiments confirmed the validity of our predictive model.

Conclusion: This study highlighted how crucial it is to deploy particle traps in an area with low current velocities, in order to limit the granulometric bias. We developed a predictive model that will be an asset to quantify particle-size distribution bias and to better understand potential particulate contaminants concentrations shifts. This work represents a significant step forward to a thorough use of PTs.

Keywords: Trapping efficiency, grain-size, monitoring, suspended particulate, matter, river

1 Introduction

Rivers form a network that drains water, sediment and pollutant from the whole landscape and transport them across territories. Human activities strongly increase particulate contaminants concentrations and their respective particulate fluxes in rivers (Wohl 2015). To prevent and manage these impacts, European directives for example, require from each Member State to monitor the contamination of hydrophobic contaminants and metals in continental surface sediments (e.g. riverbank sediment) in order to assess their temporal trends. However, the sampling of surface sediments present several operational limits, such as (i) the difficulty to collect sediment with comparable characteristics over time, due to the natural variability of sediment (e.g. particle size distribution, organic content...) or (ii) obtaining a sample with a precise datation. The sampling of suspended particulate matter (SPM) targeting small-size particles is a promising alternative to surface sediments monitoring (Schubert et al. 2012; Yari et al. 2019). Indeed, it allows to systematically collect the fine fraction (typically below 200 µm), and to obtain a precise datation of the sample.

To collect a sufficient amount of SPM for the various analyzes, continuous flow centrifugation (CFC) is often used (e.g. Burrus et al. 1989), as it provides quali- and quantitative representative samples (Harhash et al. 2023). However, CFC represents a significant investment and requires several hours of pumping/centrifugation, which makes its use difficult for large scale deployment in a monitoring network. Passive particle traps (PTs), as an alternative tool to sample SPM, are cost-efficient, easy to operate and time-integrative (Phillips et al. 2000; Masson et al. 2018). Different types of sediment samplers have been deployed, mainly in the form of boxes or tubes (such as the Phillips sampler, Phillips et al. 2000) that decrease the flow velocity to promote the settling of SPM. Sediment boxes are notably used in monitoring networks such as the German Environmental Specimen Bank (GESB, since 1995 in Germany; Schulze et al. 2007) and the Rhône Sediment Observatory (OSR, since 2011, in France; Poulier et al. 2019; Lepage et al. 2022). They were recently deployed for micro-plastic fluxes evaluation in the Danube and Rhine rivers (Kittner et al. 2022; Range et al. 2025). The Phillips sampler is also widely used around the world (Smith and Owens 2014). It was recently used for ecological studies such as microbial DNA metabarcoding (Falk et al. 2022). However, to be deployed in the field for contaminant flux estimation, the particles sampled with such traps should be representative of SPM. Several studies explored, through laboratory or field experiments, the efficiency of passive particles traps. Smith and Owens (2014) have summarized the main outcomes for the Phillips sampler evaluations, completed more recently with the work of Doriean et al. (2019) and Goharrokhi et al. (2019), and we can also cite the recent work of Harhash et al. (2023) about sediment boxes. Main conclusions were that SPM collected with these particle traps were coarser than those collected by spot sampling or by continuous pumping/centrifugation (Phillips et al. 2000; Schäfer and Blanc 2002; Pohlert et al. 2011; Smith and Owens 2014; Harhash et al. 2023) as they underestimate small particles (Harhash et al. 2023). Centrifugation is considered here as reference, as it is usually done (Masson et al. 2018) but as showed by Goharrokhi et al. (2020), it can also be subject to bias, especially for very fine particles (< 1 µm). This sampling bias for fine particles was found to be greater as the incoming flow velocity increases (Ciffroy et al. 1999; Masson et al. 2018; Doriean et al. 2019). Indeed, the higher the velocity in the PT is, the less likely to settle fine particles are. Theoretical considerations were developed for deployment of sediment trap in the ocean that can be adapted to our context (Butman et al. 1986). Dimensionless numbers

such as the ratio of particle fall velocity to surrounding flow velocity, trap height to trap mouth diameter were identified as controlling parameters.

A strategy to overcome this lack of representativity can be twofold. Because the efficiency of PTs depends on particle size and flow velocity, we can define conditions for deployment that are suitable. Harhash et al. (2023) defined what particle sizes can be effectively trapped for a specific velocity for example. It could be extended to a range of velocity. The first strategy could then be to restrict our use of PTs to such conditions. A second strategy can be to correct the PT fluxes with a law that should be predictable to get to the SPM flux (Perks et al. 2017).

Nevertheless, to the best of the authors' knowledge, there is so far no laboratory comparison with both particles of different sizes and different inflow velocity to explicit how the efficiency varies with both of these parameters jointly so that we could, for any deployment site, either determine what particles can be trapped or try to correct bias.

A trapping efficiency can be computed to qualify the PT-ability to trap the particles passing through it. It is defined as the mass ratio of the SPM captured in the PT to the SPM entering the PT. It can be considered globally, considering all particle size together, or for each particle sizes independently. When we compute this particle-size specific efficiency we not only observe a lack of fine sediments but quantify precisely which sediment are trapped so that we can predict the PSD of trapped SPM and in what conditions PTs can be deployed with limited bias. Formalizing SPM particle-size specific efficiency of PTs is a fundamental step in adapting them to limit potential biases during sampling phase and to deploy them on contrasting streams.

In order to assess the particle-size specific trapping efficiency of PTs, we designed experiments in controlled conditions. Only one type of PT was tested, the box-type PT model (deployed in GESB, and OSR; Schulze et al. 2007) and its 1:3 reduced version to explore the influence of PT size on efficiency. Experiments were carried out with flow velocities usually encountered in river sites where PTs are deployed (0.05 to 0.7 m s^{-1}) and with SPMs with particle sizes ranging from 2 to 150 µm. Three types of experiments were handled. A first set of in-line experiments (PT directly fed with water and SPM with a pipe connected to its inlet) allowed to collect accurate and consistent dataset of PT efficiency for different particle-sizes. These laboratory experiments greatly limit uncertainties, as both what enters and goes out of the PT can be quantified. Nevertheless, they are not representative of the majority of field deployment when PT is submerged in the flow. In particular, the processes (linked to particles inertia in particular) taking place in the surrounding flow when entering the PT are not reproduced. We then designed a second type of experiments in the laboratory, but with the PT submerged in a flow with SPM (in-flow experiments). In the flume we used, flow velocity and SPM concentration could be kept constant and analysis of the results simpler. Finally, the third type of experiment consisted of two field deployments conducted under low and high flow velocity and SPM concentrations.. The conditions are then more complex with varying SPM concentration and flow velocity but testing it is a mandatory step to assess our results in operational condition in rivers.

2 Methods

2.1 PT and sediment characteristics

Two PTs were tested (see Fig. 1a) to quantify scale effects. The largest PT (denoted L for large) is 400 mm-long, 250 mm-wide, 300 mm-height. It is currently in use in German Environmental Specimen Bank (Schulze et al. 2007) and OSR monitoring networks (Masson et al. 2018; Poulier et al. 2019; Delile et al. 2020). The flow can enter the PT through 3 inlets, each of 5.2 mm diameter (section $S_{\text{in}} = 8.5\ 10^{-5}\ \text{m}^2$), but only one of the 3 inlets of the L-trap was open in the following experiments as it is usually the case in the field (see Fig. 1d). This is a standard practice in our observatory as this improves trapping efficiency by reducing the flow velocity within the trap. Then, two baffles are impeding the flow within the traps (see Fig. 1d). Finally the flow gets out of the PT through the one open outlet over three. The area of the smallest cross-section within the L-trap, just below the second baffle, is $S_{\text{min}} = 1.5\ 10^{-2}\ \text{m}^2$.

The second PT we tested is a 1:3-scale trap (denoted S for small). The area of the smallest cross-section within the S-trap, also just below the second baffle, is $S_{\text{min}} = 2.0\ 10^{-3}\ \text{m}^2$. We designed the S-trap with only one inlet of same size as the inlet of the L-trap (all the other lengths are 1:3 scaled).

Two types of SPM were tested in order to explore a wide range of particle sizes typical of river applications (Agrawal and Hanes 2015; Armijos et al. 2017): a well sorted fine sand (median diameter $d_{50,1} \approx 65\ \mu\text{m}$, see PSD of SPM1 in Fig 1b), and a more poorly sorted silt ($d_{50,2} \approx 15\ \mu\text{m}$, see PSD of SPM2 in Fig 1b). It is crashed glass bought in 25 kg bags, mainly composed of silicate, with a density of $2650\ \text{kg.m}^{-3}$. Both were mixed for some experiments.

2.2 Particle size specific efficiency of the PT

2.2.1 Measurements

Quantifying particle size specific efficiency requires both SPM concentration and PSD measurements. We measured the PSD of one sample using a laser particle sizer (LISST 200X). SPM concentration was measured both by filtration (concentration denoted C') and opacity analysis of the laser particle sizer (concentration denoted C). For this last option, samples were diluted 10 times for coarse particles (PSD1) or 50 times otherwise to avoid saturation.

We compared both estimates of the concentration to assess our method and detect possible outliers. Both concentrations are found to be linearly related (Fig. 2), with errors that can be due to both the uncertainty of the measurements and the time-variation of concentration during each experiment. The experiments with concentrations that differ by more than a factor 2 were discarded from the following analysis.

The concentration (C_i) of each size-class i of the SPM is defined so that $C = \sum_i C_i$. The efficiency η of the PT can then be computed as the ratio between the concentration of the collected sediment $C_{i,\text{PT}}$ and the concentration of the suspension in the upstream flow $C_{i,\text{us}}$ for each size class i :

$$\eta_i = C_{i,\text{PT}}/C_{i,\text{us}} \tag{1}$$

or equivalently using mass continuity as

$$\eta_i = 1 - C_{i,\text{ds}}/C_{i,\text{us}} \tag{2}$$

where $C_{i,\mathrm{ds}}$ is the concentration for the size class i of what remained in suspension within the flow downstream of the PT. This downstream concentration can only be measured when PT is in-line. In this work, each size class is delimited by 36 logarithmically spaced values of diameter between 1 - 500 µm.

2.2.2 Theoretical considerations

We consider here some volume of water entering the PT. We define L_{PT} as the distance it needs to travel to go out of the PT and V_{PT} its velocity within the trap. Assuming that one particle suspended in this volume needs to fall down a vertical distance z_{PT} to settle within the PT at a velocity w_s, it will be trapped if the time it needs to settle down is smaller than the time to reach the outlet so if:

$$\frac{z_{PT}}{w_s} < \frac{L_{PT}}{V_{PT}} \tag{3}$$

That can be interpreted in term of efficiency as :

$$\begin{aligned} \eta = 1, \quad \text{if } \frac{L_{PT}}{z_{PT}} \frac{w_s}{V_{PT}} > 1, \\ \eta = 0, \quad \text{if } \frac{L_{PT}}{z_{PT}} \frac{w_s}{V_{PT}} < 1. \end{aligned} \tag{4}$$

We can then expect the trapping efficiency to depend on three parameters: the settling velocity, the flow velocity and the PT sizes.

1. The settling velocity w_s increases with the size of the particles (Soulsby 1997):

$$w_s = \frac{\nu}{d}\left(\sqrt{10.36^2 + 1.049 d^{*3}} - 10.36\right) \tag{5}$$

   where ν is the kinematic viscosity, d the particle size diameter, $d^* = d(g(\rho_s/\rho - 1)/\nu^2)^{1/3}$ the non-dimensional particle size, ρ_s the particle density, ρ the water density and g the gravitational constant.

   A larger particle means a larger settling velocity so that Eq.(3) is more likely to be fulfilled and the particle is more likely to be trapped. It results in a larger trapping efficiency.

   Please note that density also plays a role in settling velocity since lighter particles such as plastic particles fall less rapidly. This is consistent with Harhash et al. (2023) results showing that the trapping efficiency for a given size is smaller for plastic or lignin particles than for mineral particles.
2. The flow velocity within the trap V_{PT} can be estimated as a simple ratio between the discharge through the trap and the smallest flow cross-section S_{min} within the trap (below the second baffle, see Fig. 1d), or equivalently, as the product of the incoming flow velocity V and the ratio between the inlet cross-section S_{in} and S_{min}: $V_{PT} = V \times S_{\mathrm{in}}/S_{\mathrm{min}}$.

   If V increases, V_{PT} increases, hence Eq.(3) is less likely to be fulfilled and particle less likely to be trapped suggesting a lower trapping efficiency.
3. Similarly, a larger ratio $S_{\mathrm{in}}/S_{\mathrm{min}}$ (approximately 1/25 for the S-trap *vs* 1/180 for the L-trap), results in larger V_{PT} suggesting a lower trapping efficiency.

In our experiments, the two traps were proportionally scaled (except the inlet) so that z_{PT}/L_{PT} is the same in both cases. Defining a velocity ratio between settling velocity and velocity within the PT :

$$R_v = w_s/V_{PT}, \tag{6}$$

eq.(4) can be simply retrieved considering R_v greater or smaller than a constant. This simple ratio combines the effect of the size of the particles, the geometry of the PT and the incoming flow velocity. Turbulence of the flow is not accounted for in such model. We can expect that this variability in flow velocity will result in a smooth gradient between minimum and maximum efficient rather than a sharp step.

A previous theoretical study for passive traps in ocean (Butman et al. 1986) already mentioned a velocity ratio as a controlling parameter. Particle Reynolds number, trap Reynolds number, aspect ratio of the trap and particle relative density were also identified. The parameter we propose includes the aspect ratio of the trap and the velocity ratio. The other parameters could not be explored with this work.

2.3 Set-up for in-line experiments

The in-line experiments were designed to measure the influence of incoming velocity and SPM load on the mass of particles of each particle size that is collected within a PT. A sketch of the set-up is presented in Fig. 1. First, a 1 m^3 tank was filled with water and SPM. Four submerged pumps were fixed on rods into the tank to generate turbulence and keep the sediments in suspension (Vergne et al. 2021). A pipe was used to supply the PT with gravity flow taken from the tank (see Fig. 1c). The incoming flow velocity was set up by adjusting the level of the PT comparatively to the water surface level in the tank.

We fed the PT with a wide range of discharges that led to flow velocity at the inlet of PT between 0.07 m s^{-1} to 0.65 m s^{-1}. Discharge was measured at the outlet of the trap by weighting water with a scale (Fig. 1c), the incoming flow velocity was computed as the ratio between discharge and inlet section S_{in}.

Experiments are denoted S*i* or L*i* whether the experiment is handled with the small or the large trap (see Table 1). For one experiment, we either set several incoming flow velocities keeping concentration constant or set different concentrations keeping discharge constant (experiment L4 only).

We took 3 water samples immediately upstream and downstream of the PT. One sample was used to determined SPM concentration (g L^{-1} d.w.) while the other two samples were used to determine PSD.

2.4 Set-up for in-flow experiments

Two additional experiments with the PT submerged under a SPM laden flow were undertaken within a 18m-long, 1m-wide flume (see Perret et al. 2018, for a description of the flume and measurement devices).

We deployed the S-trap during 2 hours and 17 minutes, with upstream velocity of 0.04 m s^{-1} and SPM concentration of 0.3 g L^{-1}. We deployed the L-trap for the second experiment during 6 hours and 40 minutes, the upstream velocity was also of 0.04 m s^{-1} and SPM concentration of 0.1 g L^{-1}. We chose these conditions of low velocities to reproduce ideal deployment set-up (Ciffroy et al. 1999). The exposition duration was selected to trap a sufficient

amount of particles to proceed to the analyzes. Concentration was computed from manual samples filtration (based on 7 samples for the S-trap, 4 for the L-trap). We measured velocity with an ADV (Acoustic Doppler velocimeter, Vectrino, Nortek). Because output sediment concentration could not be measured, the efficiency was estimated from the particle size analysis of the particles that were captured within the PT (eq. 1).

2.5 Set-up for field deployment

In order to test the PT in field conditions, a PT was deployed during 6 hours (24th May 2016) in the Rhône River at the Jons station (Masson et al. 2018). We took advantage of the dam flushing operations in the upper Rhône to have quite stable conditions with high SPM concentrations (267 ± 15 mg L^{-1}) to collect enough particles for analysis, and with high discharges (between 1040 and 1080 m^3 s^{-1}). The flow velocity measured at the PT inlet was 0.90 ± 0.15 m s^{-1} (see Fig. 3a,b). During the PT deployment, 7 samples were collected manually (reference sampling method) close to the PT to constitute 7 representative samples of the particles passing through the river. Samples were filtered to obtain SPM concentration. The particle size analyzes performed on these 7 samples showed that the particle size distribution was constant during the event (see the superimposition of PSDs in Figure 3c). The average PSD was considered for further computations.

A second trap deployment was conducted at the same station over a period of 17 days during low water flow (daily discharge between 194 and 390 m^3 s^{-1} with low concentrations of SPM close to 5 mg L^{-1}). During the trap deployment, seven samples were regularly collected by continuous flow centrifugation approximately every three days. The PSD were similar for the first five samples and slightly coarser for the last two samples. Variability in the PSD was accounted for in further computations. Velocity was considered constant, equal to 0.04 m s^{-1}, based on measurements taken for similar discharges.

3 Results and discussion

3.1 Outcomes from in-line deployment

For each in-line experiment, the efficiency generally increases with the particle diameter (see Fig. 4a and b for S-trap and L-trap, respectively). For particle diameters above approximately $d_i = 100\,\mu m$ for the S-trap, $d_i = 40\,\mu m$ for the L-trap, the PT collects most of the particles ($\eta \approx 1$). Below $d_i = 10\,\mu m$, most of the particles are lost ($\eta \approx 0$). The results strongly vary across experiments, but the shape of each trapping efficiency curve is similar. For each trap, the smaller the incoming flow velocity, the larger the efficiency, as expected. Considering a given flow velocity and a given particle size, trapping efficiency is larger for the L-trap than for the S-trap: for example, for 20 µm particles with a flow velocity of 0.2 m s^{-1}, efficiency is approximately 0.5 for the S-trap and 1 for the L-trap (compare the light blue symbols in Fig. 4a and b). These results are consistent with the theoretical consideration we presented in section 2.2.2: efficiency increases with particle diameter, decreases with flow velocity and is larger for the larger PT.

We plotted the efficiency as a function of the velocity ratio R_v between the settling velocity of a given particle class and the flow velocity within the PT, as defined in Eq. 6 (Fig. 4c, d). Taking into account the R_v ratio (instead of diameter) reduces the dispersion of the curves

independently of the different incoming flow velocities (corresponding to the different colors) or trap size (upper or lower panels, Fig. 4). The remaining scatter can be largely attributed to uncertainties in the calculation of the efficiency and the settling velocity. The efficiency is computed from a ratio of particle size distributions that are known to be uncertain (Eshel et al. 2004).

As expected, efficiency values are quite low below a threshold of R_v that does not follow any significant trend in terms of incoming flow velocity or trap size. Above this threshold, efficiency increases up to 1, meaning that all particles entering the PT are trapped. Nevertheless, the increase is not as sharp as what was predicted by Eq.4. This slow transition between $R_v = 10^{-2}$ and $R_v = 1$ can be due to particles in the trap being randomly distributed in the PT so that they can be trapped even if Eq.3 is not fulfilled. This could also explain why the efficiency does not drop down to zero for low velocity ratios (or diameters). We do believe that trapping efficiency for smaller particles could be increased due to the entrainment of the smaller particles by the larger ones when they fall (Druitt 1995, considering that concentrations are high).

To reproduce this threshold behavior with a large transition, we fitted the efficiency with a hyperbolic tangent function (dashed black line in Fig. 4b) and found that the efficiency could be approximated by:

$$\eta_{\text{model}} = \frac{1}{2.2}\left[\tanh\left(1.5(\log_{10}(R_v) + 0.9)\right) + 1.2\right] \tag{7}$$

This curve can be used to estimate the diameter of the particles that will be trapped within a PT, considering the upstream flow velocity. In practice, using a PT of the same type as the one used for these experiments, we can expect to directly apply this formula as soon as we know what is the flow velocity entering the PT and the size of the PT inlet and the smallest flow cross-section within the trap. Two alternative fits are suggested (dotted black line in Fig. 4b) that encompasses the data, to assess the effect of the error between fits and measurements in further applications.

To validate this assumption, we did apply our formula to data published in the article of Harhash et al. (2023), where two different sediment boxes types PT and 6 types of particles where used. One PT is the same as the one used in this article, the second one was improved, adding 3 blades, enlarging the PT and diminishing the space below the blades. The results we obtained are presented in appendix (see figure A1). Except for the quartz particles of 2.6 µm, agreement between measured and predicted PSD is fairly good for this independent set of data. The two main limitations we found are most probably due to particle size distribution measurements uncertainties for very fine particles and large particles. Moreover, it is striking to see that there is no significant difference between the two sediment boxes types. Harhash et al. (2023) found a significantly greater efficiency regarding the total mass collected by the improved PT but the particle-size specific efficiency remains the same, and can also be predicted with our empirical relation.

Applying this formula to another type of PT such as the Phillips for example (Phillips et al. 2000) would probably require some adjustments of the fitted coefficients. Indeed, as stated by Phillips et al. (2000), basic hydrodynamic principles and Stoke's Law result in underestimating what particles can be retained, as dead zones in the flow are not considered but effectively trap fine sediments. These local hydrodynamic effects within the trap, which change considering

the shape of the trap, cannot be easily predicted and requires experiments to empirically derive them.

The suggested formula quantifies for one type of trap (sediment boxes) the behavior that was already observed in laboratory experiments for other passive traps : finer particles are less effectively trapped than coarser ones, high surrounding flow velocity reduces the trap efficiency, and the smaller fall velocity of particles is, the less the particles are trapped (see among others Phillips et al. 2000; Smith and Owens 2014; Doriean et al. 2019; Harhash et al. 2023). Nevertheless, to the best author knowledge, none of these studies were able to gather in one single parameter how efficiency evolves, nor to predict it.

3.2 Application to in-flow deployment

3.2.1 In a flume

Similarly to the efficiency measured in in-line experiments, efficiency for the two in-flow experiments with the two traps (S and L-traps, see Fig 5) globally increases with diameter. Larger particles are more collected in the PT than smaller ones with respect to the PSD of the SPM of the incoming flow. Nevertheless, the measured efficiency for the two in-flow experiments (solid line in Fig 5a, b) do not follow a hyperbolic tangent curve. Trend with diameter is not monotonous, which can probably be attributed to measurement uncertainties. Efficiency can be larger than 1 for coarser particles. Indeed, non-isokinetic traps oversample large particles when inflow velocities are lower than surrounding flows (Guy and Norman 1970). We did not measure inflow velocities in our experiments but we can expect, as it was measured for the Phillips sampler (Goharrokhi et al. 2019), that it is reduced comparatively to the surrounding flow. Thus, whereas the flow is deviated by the sampler, coarse particles go straight, and are more concentrated in the flow entering the PT, resulting in efficiencies larger than one. This effect is not accounted for when doing in-line experiments. The efficiency predicted with Eq.(7) (dashed line in Fig 5a, b) is shown for comparison and reveals a comparable threshold value of the particle size for the efficiency to increase significantly.

For both experiments, as expected, PT sample (solid red line in Fig. 5e, f) is coarser than SPM (solid black line in Fig. 5c, d): the finer peak at 3 µm is reduced and the second peak at 10 µm shifted towards 20 µm. Using Eq.(7), we can compute the PSD of sediments in the trap (dashed red line in Fig. 5e, f) as the product of the PSD of incoming SPM and the predicted efficiency η_{model} (dashed line in Fig 5a, b). The computed PSD of sediments in the PT reproduces well the measured PSD. To better assess for uncertainties in the efficiency evaluation, we also computed PSD from the two alternative fits represented in Fig. 4 as dotted lines. First, we can see that the scatter of the in-line experiments does not explain the gap between the efficiency we measured in the flume and eq. 7 (see Fig 5a, b). Second, the measured PSDs for both upstream and PT samples fall within the two PSD obtained with these two curves (see Fig 5a, b). Thus, the slight differences between PSD can be explained by uncertainties in the efficiency fit.

Conversely, the PSD of the incoming SPM can be computed from the PT-sample PSD. Again, we were able to reproduce the SPM PSD with our computation, retrieving a fine peak at 3 µm and the shift to finer sediment for the second peak.

Although the model does not perfectly reproduce the efficiency measured during the in-flow experiments as processes occurring at the inlet are disregarded, it nevertheless allows fairly

accurate prediction of the PSD of the incoming SPM from the PSD of PT samples, and vice-versa. Trying to analyze directly particle-size dependent efficiency for in-flow experiments is hazardous and the preliminary step of in-line experiments analysis was proven to be useful to understand and quantify the particle size bias in the sediment collection using PTs.

3.2.2 In the Rhône River, France

During the dam flushing event in the Rhône River, France, SPM concentration and velocity (0.69 - 1.06 m s^{-1}) changed slightly during the deployment (see Figure 3), so we computed for each time step the mass per class size collected by the PT using eq. (7). We computed the sum of these masses to obtain the particle size distribution of the virtually collected mass. This predicted PSD can be compared to the PSD of the PT sample in Fig. 6a. PSD of the SPM in the incoming flow is recalled for comparison. As previously mentioned in the literature, PT seems to miss the finest particles and PSD of the PT sample is significantly coarser than PSD of the SPM upstream. This reduced proportion of fine sediment within the PT is well predicted applying the efficiency model developed with the in-line experiments. It results in higher proportion of coarser particles of about 30 µm, which is also well predicted.

The same methodology was applied to a PT deployment during low flows. Results are presented in Fig. 6b. For such low flows and low concentration, eq. (7) over-predicts the loss of fine particles by the PT. We do believe that for such long durations of sampling, with low velocities and very low SPM concentration ($\approx$ 5 mg L^{-1}), the processes in the PT might be probably different, the recirculation zones within the PT having a greater impact on the total mass collected.

These results are consistent with what was already observed in the field, either for this same box-type PT (Masson et al. 2018), or for other PT types (Phillips et al. 2000; Schäfer and Blanc 2002; Perks et al. 2014; Smith and Owens 2014; Doriean et al. 2019). The application of Eq. (7) to varying concentration and velocity is useful to analyze what was collected with a PT for high velocity flows.

4 Conclusion

This experimental work successfully characterized the particle-size specific efficiency of SPM collected by particle traps commonly used for the monitoring of fine particles and associated contaminants in river systems.

Using in-line experiments, with the PT fed with a pipe, we suggested a simple semi-empirical model for the particles settling within the PT and revealed that the trapping efficiency can be predicted from the ratio between the settling velocity of a given particle class and the flow velocity within the PT. This flow velocity can be easily estimated using the surrounding flow velocity and the PT dimensions. We quantified how an increase in incoming flow velocity decreases the proportion of the finer particles that are effectively trapped. This empirical formula was fitted for a box-type PT and silt particles but its derivation is based on simple physical considerations so that it should be easily adapted to other types of PT. It was applied successfully to particles of lignin (with different density) so should be also easily adapted for other types of particles (such as plastics or organic matter). We can add that a modification of design such as the addition of a blade, does effectively increase the overall efficiency of the trap but seems to have no effect on the particle-size specific efficiency (Harhash et al. 2023).

We applied this model to in-flow experiments where the PT was submerged in a Suspended Particulate Matter (SPM)-laden flow. It allows a fairly good prediction of the PSD of incoming SPM from the PSD of PT samples, or the PSD of PT samples from the PSD of incoming SPM. Similar application was also handled in the Rhône River with also good results when deployment is for short period, with high levels of concentration and velocity. For lower velocities ($\approx 0.2\,\mathrm{m\,s^{-1}}$), very low concentrations ($\approx 5\,\mathrm{mg\,L^{-1}}$) and long period of deployment, the empirical relation predicts low efficiency for small particles ($< 1\,\mu\mathrm{m}$) but we observed almost no bias for the PT.

Further applications could be twofold. On the one hand, assuming that we want to monitor the fine particles of a given stream with a given trap, at a specific location with a given flow velocity and PSD of suspended sediment, we can use this efficiency model to know what particles can be trapped. Conversely, we can adjust the PT size or deployment location to sample particles as fine as a given diameter. We provide, for the L-PT we used which correspond to a sedimentation box widely use (Schulze et al. 2007; Poulier et al. 2019; Kittner et al. 2022; Lepage et al. 2022), an abacus to easily estimate for a range of velocity, the size of the particles that can be trapped (see Figure 7). Our results further highlight how crucial it is to deploy traps in a protected area with very low flow velocities. These areas are often found on the side of the river, behind obstacles, and can be detected using velocimeters or visually with some tracer (e.g. wood stick) for example.

On the other hand, if we deployed one PT in a river and we know what was the incoming velocity, the particle size distribution of particles in suspension in the incoming flow can be estimated from what was sampled by the PT. With this work, we also developed a method to quantify a PT efficiency, depending on its basic characteristics: travel distance, cross-section ratio. We could apply this method to other types of PT and further improve a PT design with a reliable metric to optimize.

Considering that contaminant levels depend on particle size, it is essential to know what fine particles we could have missed with the PT samples. The predicted efficiency could be used to correct contaminant levels provided that we know the particle-size vs contaminant concentration relation and that other processes such as degradation or reaction within the PT are negligible.

Funding Declaration. This study was carried out thanks to the Rhône Sediment Observatory (OSR), a multi-partner research program funded through the Plan Rhône-Saône by the European Regional Development Fund (ERDF), Agence de l'eau RMC, CNR, EDF and three regional councils (Auvergne-Rhône-Alpes, PACA and Occitanie). OSR is part of a scientific network including the Rhône Valley Human-Environment Observatory (OHM) and Rhone Basin Workshop Area (ZABR).

Acknowledgments. We gratefully acknowledge the reviewers for their contribution in improving our article. We gratefully acknowledge Lars Duester for enlightening discussions and sharing the data of Harhash et al. (2023). We gratefully acknowledge the following INRAE colleagues for SPM sampling, sample analysis, data analysis or discussions: Alexis Buffet, Mickaël Lagouy, Chloé Le Bescond, Loïc Richard, Alexandra Gruat and Benoît Camenen.

Competing Interest declaration. All authors have no conflicts of interest.

Author Contribution declaration. C. Berni, Y. Bonenfant, F. Thollet, M. Masson, A. Dabrin and J. Le Coz conceived and planned the experiments. Y. Bonenfant, F. Thollet and C.

Berni carried out the experiments. F. Thollet and Y. Bonenfant contributed to sample analysis. C. Berni, Y. Bonenfant, J. Le Coz, M. Masson contributed to the interpretation of the results. C. Berni took the lead in writing the manuscript. All authors provided critical feedback and helped shape the research, analysis and manuscript.

References

Agrawal Y, Hanes D (2015) The implications of laser-diffraction measurements of sediment size distributions in a river to the potential use of acoustic backscatter for sediment measurements. Water Resour Res 51:8854–8867

Armijos E, Crave A, Espinoza R, et al (2017) Measuring and modeling vertical gradients in suspended sediments in the Solimões/Amazon River. Hydrol Process 31:654–667

Burrus D, Thomas R, Dominik J, et al (1989) Recovery and concentration of suspended solids in the upper rhone river by continuous flow centrifugation. Hydrol Process 3(1):65–74

Butman CA, Grant WD, Stolzenbach KD (1986) Predictions of sediment trap biases in turbulent flows: a theoretical analysis based on observations from the literature. J Mar Res 44:601–644

Ciffroy P, Vazelle D, Mataix V, et al (1999) Comparison of methods for sampling suspended matter in rivers: application to measurement of particulate metals. Hydroécologie Appliquée 11:71–102

Delile H, Masson M, Miège C, et al (2020) Hydro-climatic drivers of land-based organic and inorganic particulate micropollutant fluxes: The regime of the largest river water inflow of the mediterranean sea. Water Res 185:116067

Doriean N, Teasdale P, Welsh D, et al (2019) Evaluation of a simple, inexpensive, in situ sampler for measuring time-weighted average concentrations of suspended sediment in rivers and streams. Hydrol Process 33(5):678–686

Druitt T (1995) Settling behaviour of concentrated dispersions and some volcanological applications. J Volcanol Geotherm Res 65(1-2):27–39

Eshel G, Levy G, Mingelgrin U, et al (2004) Critical evaluation of the use of laser diffraction for particle-size distribution analysis. Soil Sci Soc Am J 68:763–743

Falk N, Droppo I, Drouillard K, et al (2022) Integrating microbial dna community analyses into time-integrated suspended sediment sampling methods. J Soils Sediments 23:3574–3588

Goharrokhi M, Pahlavan H, Lobb D, et al (2019) Assessing issues associated with a time-integrated fluvial fine sediment sampler. Hydrological Processes 33(15):2048–2056

Goharrokhi M, Lobb DA, Owens PN (2020) Evaluation of high-flow rate continuous-flow centrifugation and filtration devices for sampling and concentrating fine-grained suspended

sediment. Hydrological Processes 34(19):3882–3893

Guy H, Norman V (1970) Field methods for measurement of fluvial sediment, vol 5. US Government Printing Office

Harhash M, Schroeder H, Zavarsky A, et al (2023) Efficiency of five samplers to trap suspended particulate matter and microplastic particles of different sizes. Chemosphere 338:139479

Kittner M, Kerndorff A, Ricking M, et al (2022) Microplastics in the danube river basin: A first comprehensive screening with a harmonized analytical approach. ACS ES&T Water 2(7):1174–1181

Lepage H, Gruat A, Thollet F, et al (2022) Concentrations and fluxes of suspended particulate matter and associated contaminants in the rhône river from lake geneva to the mediterranean sea. Earth Syst Sci Data 14(5):2369–2384

Masson M, Angot H, Le Bescond C, et al (2018) Sampling of suspended particulate matter using particle traps in the Rhône River: relevance and representativeness for the monitoring of contaminants. Sci Total Environ 637-638:538–549

Perks M, Warburton J, Bracken L (2014) Critical assessment and validation of a time-integrating fluvial suspended sediment sampler. Hydrol Process 28:4795–4807

Perks M, Warburton J, Bracken L, et al (2017) Use of spatially distributed time-integrated sediment sampling networks and distributed fine sediment modelling to inform catchment management. J Environ Manage 202:469–478

Perret E, Berni C, Camenen B, et al (2018) Transport of moderately sorted gravel at low bed shear stresses: The role of fine sediment infiltration. Earth Surf Processes Landf 43(7):1416–1430

Phillips J, Russell M, Walling D (2000) Time-integrated sampling of fluvial suspended sediment: a simple methodology for small catchments. Hydrol Process 14(14):2589–2602

Pohlert T, Hillebrand G, Breitung V (2011) Effects of sampling techniques on physical parameters and concentrations of selected persistent organic pollutants in suspended matter. J Environ Monit 13:1579–1588

Poulier G, Launay M, Le Bescond C, et al (2019) Combining flux monitoring and data reconstruction to establish annual budgets of suspended particulate matter, mercury and pcb in the rhône river from lake geneva to the mediterranean sea. Sci Total Environ 658:457–473

Range D, Kamp J, Dierkes G, et al (2025) A critical view on determination of annual microplastic loads in the rhine river. Water Research 283:123835

Schubert B, Heininger P, Keller M, et al (2012) Monitoring of contaminants in suspended particulate matter as an alternative to sediments. TrAC Trends in Analytical Chemistry 36:58–70. Chemical Monitoring Activity for the Implementation of the Water Framework

Directive

Schulze T, Ricking M, Schröter-Kermani C, et al (2007) The german environmental specimen bank, sampling, processing, and archiving sediment and suspended particulate matter. J Soils Sediments 7:361–367

Schäfer J, Blanc G (2002) Relationship between ore deposits in river catchments and geochemistry of suspended particulate matter from six rivers in southwest france. Sci Total Environ 298:103–118

Smith TB, Owens PN (2014) Flume- and field-based evaluation of a time-integrated suspended sediment sampler for the analysis of sediment properties. Earth Surf Processes Landf 39(9):1197–1207

Soulsby R (1997) Dynamics of marine sands: a manual for practical applications. Thomas Telford Publications

Vergne A, Berni C, Le Coz J, et al (2021) Acoustic backscatter and attenuation due to river fine sediments: Experimental evaluation of models and inversion methods. Water Resour Res 57(e2021WR029589)

Wohl E (2015) Legacy effects on sediments in river corridors. Earth Sci Rev 147:30–53

Yari A, Dabrin A, Coquery M (2019) Methodology for the evaluation of temporal trends of contaminants concentrations in sediments and suspended solids in continental aquatic systems. Techniques - Sciences - Methodes 114(6):71–84

Appendix A Application to published data

To further validate our empirical relation, we applied our empirical relation for efficiency to experimental data of Harhash et al. (2023). Indeed, they did in-line experiments similar to the one presented in this article using a single discharge to feed the PT but 6 different types of particles and 2 different sediment bow type PT (SB2 and SB3). Particle types included various sizes and lighter particles of lignin. The SB2 sediment box is the same as the one used in this article. The second one (SB3) present 5 blades (instead of 2), is larger (length x height x width of 60 cm × 20 cm x 45 cm), with a space between bottom and baffle of 26 mm, leading to a smallest cross-section within the SB3 trap of $S_{\mathrm{min,SB3}} = 1.17\ 10^{-2}\ \mathrm{m}^2$.

The PSD of the particles fed into the PT, along with what was measured within the PT and what eq.7 predicted to be trapped are presented in figure A1, for the 6 types of particles tested. Further details concerning experiment details of particles specifications can be found in Harhash et al. (2023).

Table 1 Upstream conditions (incoming flow velocity V and upstream SPM concentration C_{up}) for in-line experiments Li with the large PT and Si with the small PT. SPM1 and SPM2 are the two types of SPM used in this study, with their PSD presented Fig. 1b.

Exp.	SPM	V (m s^{-1})	C_{up} (g L^{-1})	Exp.	SPM	V (m s^{-1})	C_{up} (g L^{-1})
L1	SPM2	0.57	3.4	**S1**	SPM1	0.21	0.9
		0.44	3.1			0.13	0.3
		0.37	2.8			0.07	0.3
		0.19	7.4				
L2	SPM1	0.57	3.8	**S2**	SPM1	0.54	0.3
	+	0.46	3.3			0.42	0.1
	SPM2	0.37	3.4			0.35	unknown
		0.19	9.8			0.29	0.1
L3	SPM1	0.55	2.9	**S3**	SPM2	0.66	3.9
	+	0.44	2.5			0.51	3.5
	SPM2	0.36	3.2			0.24	5.1
		0.21	3.9			0.13	7.2
L4	SPM1	0.38	2.9				
	+	0.38	1.0				
	SPM2	0.38	0.8				
		0.38	0.4				

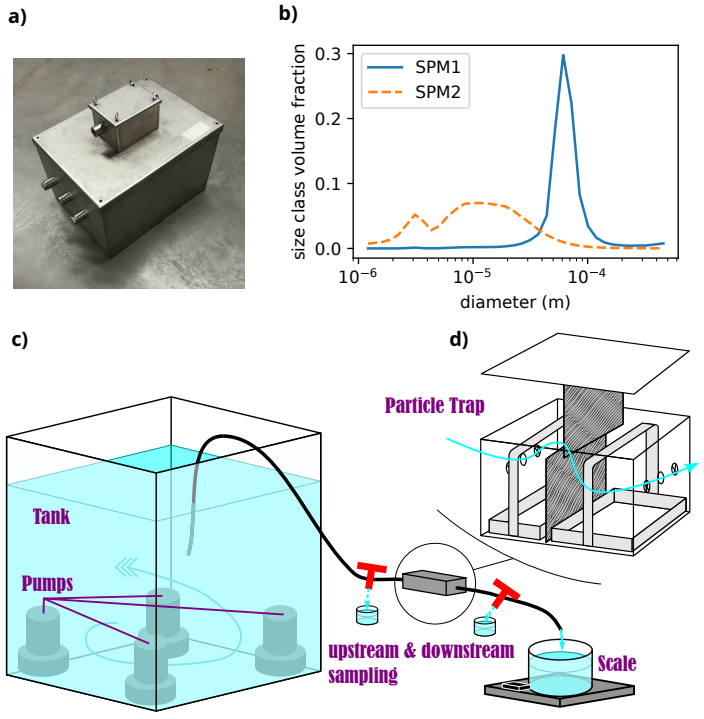

Fig. 1 Laboratory experiments and particle traps (PT) specifications: a) Picture of the two PTs. b) Particle size distribution for the two types of SPM used (SPM1; $d_{50,1} \approx 65\,\mu$m and SPM2; $d_{50,1} \approx 15\,\mu$m). c) Set-up for the calibration experiments of the PT. d) Schematic representation of a PT.

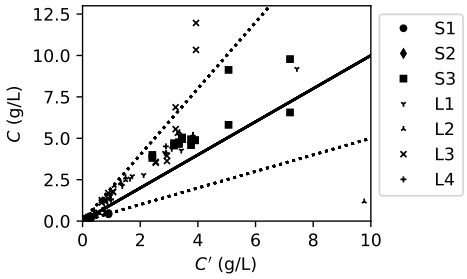

Fig. 2 Comparison of concentrations obtained by filtration (C') and laser particle sizer (C) for in-line experiments with large (denoted Li) and small (denoted Si, see table 1 for conditions of experiments). Black line stand for equality, dashed lines a factor 2 error. Coefficient of determination for a linear regression is $R^2 = 0.7$.

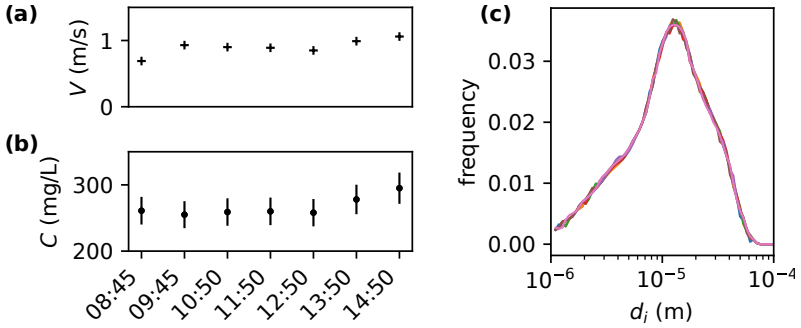

Fig. 3 Conditions during the dam flush operation of the Rhône River. Time series of (a) Velocity V and (b) concentration C with relative error bars estimated to 8 %. (c) PSD of the 7 manual samples.

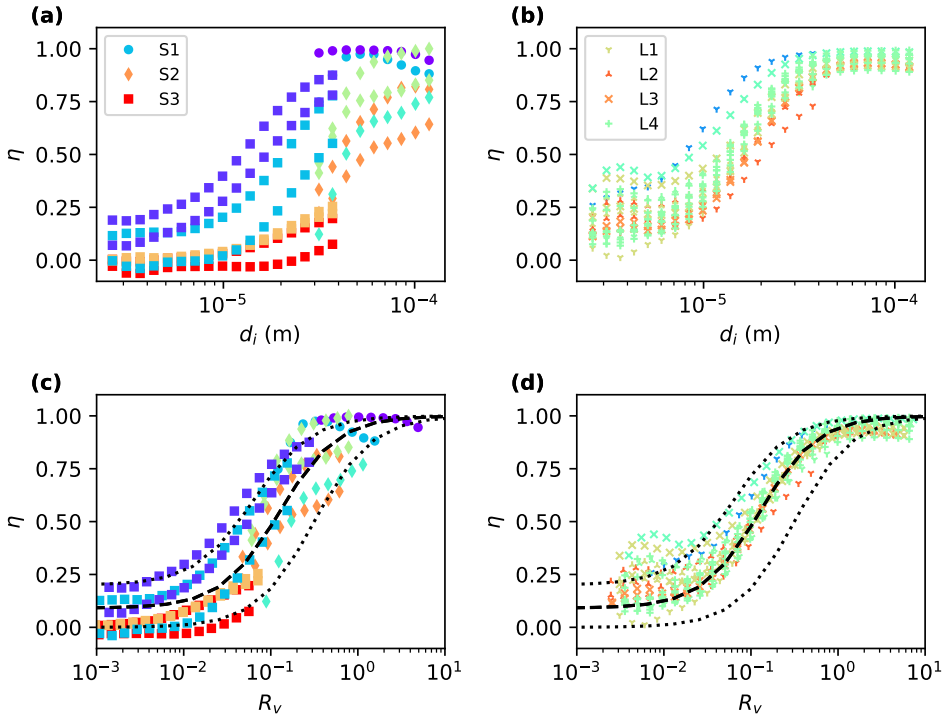

Fig. 4 Trapping efficiency η of the PT vs sediment diameter d_i (a) for S-trap experiments (b) for L-trap experiments (see table 1 for conditions for Si and Li experiments) ; Trapping efficiency η of the PT vs velocity ratio R_v (c) for S-trap experiments (d) for L-trap experiments. Hyperbolic tangent function fit (eq. 7, dashed black line) and alternative fits applied in fig. 5 (dotted black line).

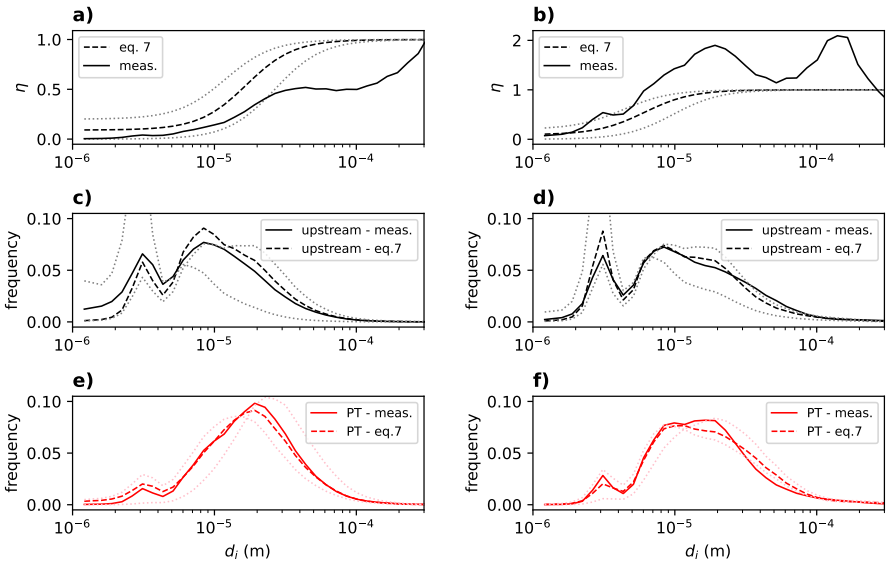

Fig. 5 In-flow flume experiments: particle-size sampling efficiency of the S-trap (a) and L-trap (b). Relative particle size distributions of SPM (black lines) for the S-trap (c) and L-trap (d). Relative particle size distributions of PT sample (red lines) for the S-trap (e) and L-trap (f). Solid lines correspond to measured values, dashed lines to computed values using the formula derived from in-line experiments for efficiency (see eq. 7). Dotted lines are relative to alternative fits for efficiency figuring as a dotted lines in fig. 4.

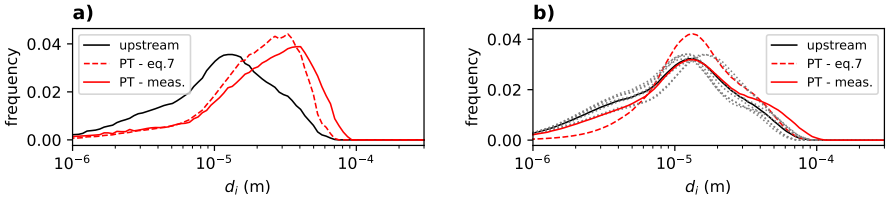

Fig. 6 Mean relative particle size distributions of upstream samples (black line) and sediment deposit in the PT (red lines): a) Rhône dam flushing event: b) Low water flow period. Solid lines correspond to measured values, dashed line to computed PSD using the formula derived from in-line experiments for efficiency (see eq. 7). The 7 PSD from centrifugation samples measured during the period of deployment for low flow stands in gray dotted lines.

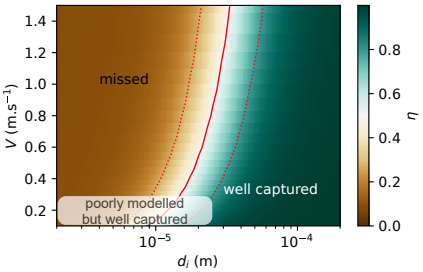

Fig. 7 Abacus for particle-size efficiency of the L-PT as function of diameter d_i and flow velocity V. Green stands for full efficiency whereas brown stands for none of the particles being trapped. Red curves mark the diameter for which efficiency is 0.5 with eq. 7. Red dotted lines mark this same diameter for alternative fits in dotted lines in figure 4.

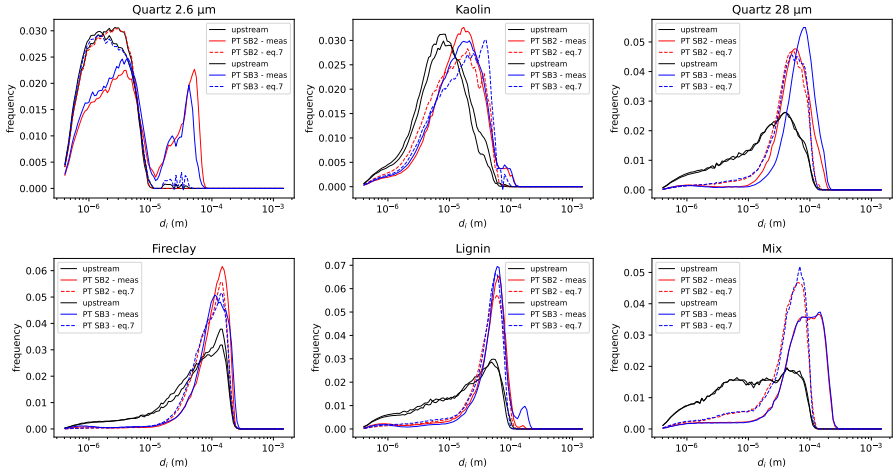

Fig. A1 Experiments published in Harhash et al. (2023): Mean relative particle size distributions of upstream samples (black lines) and sediment deposit in the SB2-PT (red lines) and SB3-PT (blue lines). Solid lines correspond to measured values, dotted line to computed PSD using the formula derived from in-line experiments for efficiency (see eq. 7).